

The Interplay of Electrostatic Interactions and Hydrophobic Hydration at the Surface of Tetra-n-alkylammonium Bromide Solutions

S. Strazdaite,* J. Versluis, and Huib J. Bakker*

FOM Institute Amolf, Science park 102, Amsterdam 1098 XG, The Netherlands

E-mail: strazdaite@amolf.nl; bakker@amolf.nl

Abstract

We use intensity and heterodyne-detected vibrational sum-frequency generation (VSFG and HD-VSFG) to study the structure of water at the surface of aqueous tetra-n-alkylammonium bromide (TAABr) solutions. We compare the water structure for four different n-alkyl chains ($n = 1, 2, 3, 4$). For solutions of tetra-n-alkylammonium bromides with short n-alkyl chains ($n = 1, 2$), we observe the structure of the surface water to be similar to the structure observed for simple inorganic salt solutions. For these solutions, the presence of Br^- at the interface is observed to lead to a small decrease in the average strength of the hydrogen bonds. For solutions of tetra-n-alkylammonium bromides with long n-alkyl chains ($n = 3, 4$), we observe a strong ordering of the water molecules at the solution surface. The water molecules show a net orientation of their O-H group towards the bulk, which can be explained from the high surface propensity of positively charged tetra-n-alkylammonium ions with long alkyl chains ($n = 3, 4$). With increasing concentration of TAABr this ordering decreases and at very high concentrations ($> 2 \text{ M}$) the orientation of the water molecules reverses. This latter finding

*To whom correspondence should be addressed

1
2
3
4
5
6
7
8
9
10
11
12
13
14
15
16
17
18
19
20
21
22
23
24
25
26
27
28
29
30
31
32
33
34
35
36
37
38
39
40
41
42
43
44
45
46
47
48
49
50
51
52
53
54
55
56
57
58
59
60

can be explained from the formation of aggregated clusters of TAA⁺ cations and Br⁻ anions near the solution surface.

Introduction

Hydrophobic interactions play an essential role in several biological phenomena, such as protein folding and the formation of biological membranes.¹ This interaction is governed by the thermodynamics of the hydration of hydrophobic molecular groups. These thermodynamics show a remarkable dependence on the size of the hydrophobic solute. In particular, for small solutes with a typical size <1 nm, the entropy of hydration is negative, which indicates that small solutes are well accommodated in water, leading to an enhancement of the water structure and hydrogen-bonding network. In contrast, large solutes disrupt the water structure, leading to the formation of a vapour-like interface. An elegant theoretical description of this length-scale dependence was developed by Lum, Chandler and Weeks.^{2,3}

Tetra-n-alkylammonium halides (TAAX, X = Br⁻, Cl⁻ and etc.) are widely used as model systems to study hydrophobic phenomena, because the tetra-alkyl-ammonium (TAA) ion is well soluble in water and its hydrophobicity can be tuned by varying the length of the alkyl chain. TAA⁺ ions display both electrostatic and hydrophobic interactions. A number of studies have been performed on TAA salt solutions to investigate hydrophobic hydration and in particular the cross-over behavior of small and large hydrophobic solutes. Early thermodynamic and transport studies have pointed indirectly to an increased ordering of water around large TAA⁺ cations such as tetrapropylammonium (TPA) and tetrabutylammonium (TBA).^{4,5} In contrast to that, a later neutron diffraction study of TAABr solutions found that the hydrogen-bond structure of water around TAA⁺ cations does not differ from that of bulk water, meaning that the structural enhancement of water commonly associated with hydrophobic hydration was not observed.^{6,7} Recent small-angle x-ray scattering experiments did find the water structure around the hydrophobic TAA⁺ ions to be enhanced compared to

1
2
3 bulk water. This enhancement was observed to be more pronounced for TPABr and TBABr
4 solutions than for tetramethylammonium bromide (TMABr) and tetraethylammonium bro-
5 mide (TEABr) solutions.⁸
6
7
8

9
10 With most spectroscopic techniques such as infrared or Raman, it is challenging to mea-
11 sure the effect of hydrophobic moieties on the structure of water, because the contribution
12 of the hydration shells to the signal is usually much smaller than the bulk water signal.
13 Here we use the surface-specific technique of vibrational sum-frequency generation (VSFG)
14 spectroscopy to study the effects of TAA⁺ and Br⁻ ions on the hydrogen-bond structure of
15 water. In the dipole approximation, VSFG only yields a signal for systems that lack inversion
16 symmetry. As a result, VSFG spectroscopy of aqueous solutions of TAABr yields a signal
17 that specifically represents the structure of the water molecules at the solution surface.
18
19
20
21
22
23
24
25
26
27

28 Experimental

29
30
31 In the present work we use both intensity VSFG and heterodyne-detected VSFG (HD-
32 VSFG). The latter technique allows the determination of the water orientation at the inter-
33 faces.⁹⁻¹¹ Details of our experimental setups have been given elsewhere.^{12,13} Briefly: part of
34 the output of commercial Ti:sapphire amplifier system (~ 3.5 mJ, 35 fs, 800 nm) is used to
35 pump a home-built optical amplifier (OPA) to generate a broad-band mid-IR pulse centered
36 at ~ 3 μm (~ 10 μJ , bandwidth ~ 300 cm^{-1}). The remaining part of the 800 nm pulse is
37 spectrally narrowed, and focused together with the broad-band IR pulse to generate light
38 at the sum frequency at the sample surface. The generated SFG light is detected with an
39 Electron-Multiplied Charge Coupled Device (EMCCD, Andor Technologies). In the HD-
40 VSFG setup, a broad-band IR pulse and a narrowband 800 nm pulse are focused first on a
41 metal surface (gold) to generate a local oscillator SFG (LO-SFG) beam. Next the LO-SFG
42 and the remaining IR and VIS beams are refocused onto the sample, producing a VSFG
43 signal that interferes with the LO-SFG. All spectra in this paper were recorded with ssp
44
45
46
47
48
49
50
51
52
53
54
55
56
57
58
59
60

polarization combination (s-SFG, s-VIS, p-IR). The spectra are normalized to a reference SFG spectrum measured from z-cut quartz.

In the preparation of the samples we used water from a Millipore Nanopure system (18.2 M Ω cm). TMABr (≥ 98 %), TEABr (≥ 99 %), TPABr (≥ 98 %), TBABr (≥ 99 %), and TPACl (≥ 98 %) were purchased from Sigma Aldrich and used without further purification.

Results and Discussion

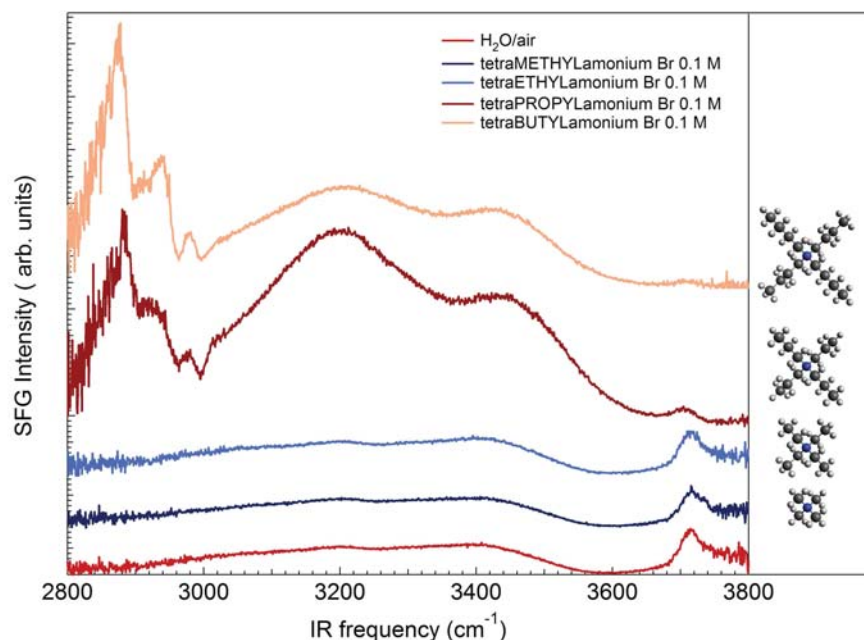


Figure 1: Intensity V-SFG spectra of pure water and 0.1 M tetra-n-alkylammonium bromide salt solutions.

Figure 1 shows intensity SFG spectra of neat water and different 0.1 M concentration tetra-n-alkylammonium bromide (TAABr) solutions. The neat water/air spectrum consists of a broad spectral feature in the 3000 - 3600 cm^{-1} region and a sharp feature at 3700 cm^{-1} . The broad feature represents the response of hydrogen-bonded O-H groups. This band is inhomogeneously broadened, representing a large variety of hydrogen-bond structures and

1
2
3 hydrogen-bond strengths. Because of the strong intra- and intermolecular coupling of the
4 O-H stretch vibrations, there is not a one-to-one correspondence between the strength of
5 the donated hydrogen bond and the O-H stretch frequency. Nevertheless, strong hydrogen
6 bonds correlate with low O-H stretch vibrational frequency and weak hydrogen bonds with
7 high O-H stretch frequencies. The broad response contains a subtle substructure with two
8 maxima at $\sim 3200\text{ cm}^{-1}$ and $\sim 3400\text{ cm}^{-1}$. This substructure has been explained from the
9 coupling of the symmetric OH stretch vibration and the overtone of the bending mode,¹⁴
10 giving rise to a weak Evans window at the frequency of the bending overtone of $\sim 3300\text{ cm}^{-1}$.
11 A change in hydrogen-bond strength will lead to a shift of the broad feature and thus to a
12 change in the relative intensities of the maxima at 3200 and 3400 cm^{-1} . The narrow peak
13 at $\sim 3700\text{ cm}^{-1}$ is assigned to non-hydrogen-bonded OH groups and originates from water
14 molecules for which one of the OH groups is sticking out of the surface.
15
16
17
18
19
20
21
22
23
24
25
26
27

28 The VSFG spectra of 0.1 M concentration tetra-methyl-ammonium bromide (TMABr)
29 and tetra-ethyl-ammonium bromide (TEABr) solutions are practically indistinguishable from
30 the pure water spectrum. In contrast, the VSFG spectra of tetra-propyl-ammonium bromide
31 (TPABr) and tetra-butyl-ammonium bromide (TBABr) are quite different. The VSFG spec-
32 tra of TPABr and TBABr solutions show a clear response in the spectral region of the CH
33 stretch vibrations ($2800 - 3100\text{ cm}^{-1}$) that is not observed for the TMABr and TEABr solu-
34 tions and also show a much higher intensity than the VSFG spectrum of bulk water in the
35 O-H vibrational region. These observations indicate that TAA⁺ ions with long alkyl chains
36 ($n = 3, 4$) have a much higher surface propensity than TAA⁺ ions with short alkyl chains
37 ($n = 1, 2$).
38
39
40
41
42
43
44
45
46
47

48 In Figure 2 we present VSFG spectra of solutions of TEABr and TPABr at different
49 concentrations. For TEABr (Figure 2a) the VSFG intensity shows a gradual increase with
50 concentration, and there is no significant change in the shape of the spectrum, except for a
51 small blue-shift at the highest measured concentration of 8 M. For TPABr the VSFG intensity
52 strongly increases with concentration. At a bulk concentration of $\sim 0.001\text{ M}$ of TPABr, the
53
54
55
56
57
58
59
60

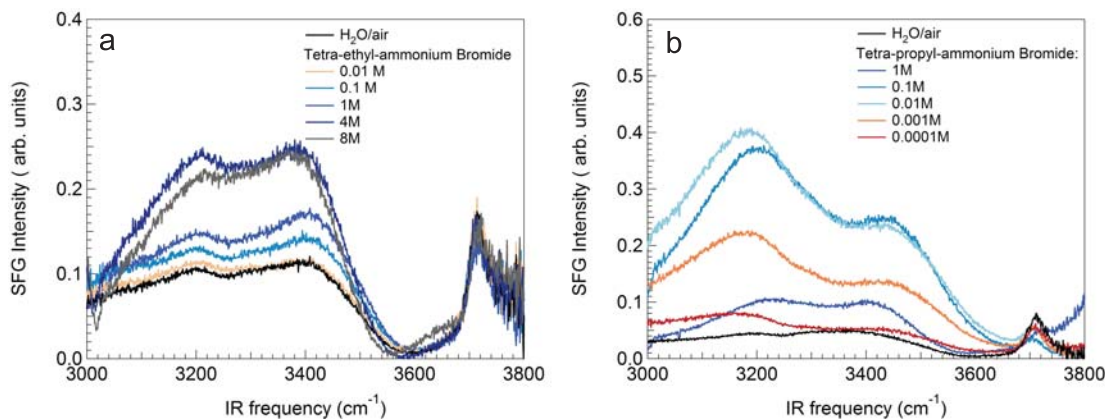


Figure 2: Intensity VSFG spectra of (a) TEABr and (b) TPABr salts at different concentrations.

VSFG intensity is already substantially higher than that of pure water. The VSFG intensity reaches a maximum value at a low bulk concentration of ~ 0.01 M: a further increase of the concentration leads to a decrease of the VSFG signal. Besides the clear intensity changes, the addition of TPABr is observed to lead to a red-shift of the broad hydrogen bonded water band. Up to concentrations of 1 M, the low-frequency peak (~ 3200 cm^{-1}) is much stronger than the high-frequency peak (~ 3400 cm^{-1}), which is quite different from the VSFG signal of the surface of pure water, for which the two peaks are of approximately equal intensity.

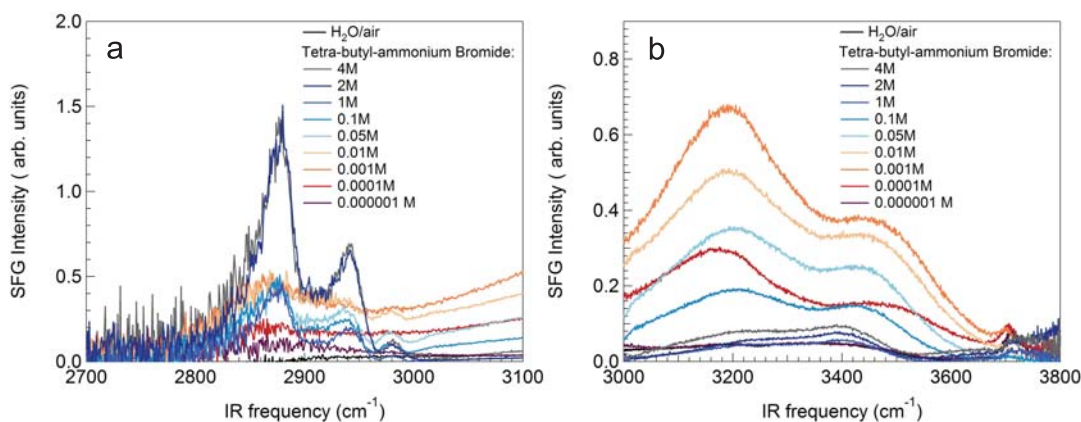


Figure 3: Intensity VSFG spectra of solutions at different concentrations of TBABr in H_2O . (a) Frequency region of the C-H stretch vibrations, and (b) frequency region of the O-H stretch vibrations.

In Figure 3 we present VSFG spectra of solutions of TBABr at different concentrations.

1
2
3
4 In Figure 3a we probe the C-H stretch vibrational region and here we observe a gradual
5 increase of the bands at 2865 cm^{-1} , 2940 cm^{-1} and 2980 cm^{-1} . We assign these bands to
6 the symmetric C-H stretch vibration, the Fermi resonance and the asymmetric C-H stretch
7 vibration of the CH_3 groups of the butyl chains, respectively. In Figure 3b we probe the O-H
8 stretch vibrational region of the interfacial water molecules. The VSFG spectra of TBABr
9 solutions show a very similar shape and concentration dependence as the VSFG spectra of
10 TPABr solutions in the same frequency region (Figure 2b). For TBABr the VSFG signal
11 reaches a maximum intensity at an even lower concentration ($\sim 0.001\text{ M}$ for TBABr and
12 $\sim 0.01\text{ M}$ for TPABr), which indicates that TBABr has an even higher surface propensity
13 than TPABr. For concentrations $> 0.001\text{ M}$ the VSFG signal of TBABr solutions starts to
14 decrease and at $\sim 1\text{ M}$ the VSFG spectrum in the O-H region looks quite similar to that of
15 pure water. Finally, at higher concentrations ($> 1\text{ M}$) the spectrum shows a slight increase
16 again and the high-frequency peak of the O-H stretch spectrum becomes larger than the
17 low-frequency peak.
18
19
20
21
22
23
24
25
26
27
28
29
30
31

32 The concentration range of the VSFG spectra of TPABr and TBABr solutions in the O-H
33 stretch vibrational region can thus be divided into three regions: a low concentration range
34 (0 - 0.01 M), in which the VSFG signal strongly increases and red shifts, indicating that
35 the water molecules at the surface become much more oriented and more strongly hydrogen
36 bonded; a medium concentration range (0.01 - 1 M), where the VSFG signal decreases and
37 becomes less red-shifted, which means that the water molecules become less oriented and
38 less strongly hydrogen bonded; and a high concentration range (1 - 4 M), where the VSFG
39 signal again slightly increases and the spectral response gets blue-shifted, indicating that the
40 probed water molecules are more weakly hydrogen bonded.
41
42
43
44
45
46
47
48
49

50 The red-shift of the VSFG spectrum of the O-H stretch vibrations is a quite interesting
51 observation. Infrared absorption spectra of TBABr solutions that probe the response of
52 the bulk water molecules do not show such a red-shift of the response of the O-H stretch
53 vibrations (see Figure SI1). In fact, the infrared absorption shows a blue-shift of the O-H
54
55
56
57
58
59
60

1
2
3 stretch absorption band that gets more pronounced with increasing concentration. The blue
4 shift can be explained from the fact that the hydrogen bonds between water molecules and
5 bromide ions are weaker than water-water hydrogen bonds. As a result, the O-H stretch
6 vibrations of water molecules hydrating the Br^- ions appear at higher frequencies (blue-
7 shifted).¹⁵ The Raman spectra of TMACl, TEACl and TPACl also show an enhancement of
8 the high frequency water peak, which is explained from the formation of hydrogen bonds to
9 Cl^- ions that are weaker than the hydrogen bonds between water molecules.¹⁶ Clearly, the
10 red shift of the O-H stretch VSG response of low-concentration solutions of TPABr and
11 TBABr solutions is quite anomalous and likely a highly surface-specific phenomenon.

21 To investigate the effect of TAABr salts on the orientation and hydrogen bonding of
22 surface water molecules in more detail, we performed HD-VSG experiments. In Figure 4
23 we present the imaginary part of $\chi^{(2)}$ ($\text{Im } \chi^{(2)}$) for the surfaces of pure water and tetra-
24 n-alkylammonium bromide ($n = 1, 2, 3, 4$) solutions at different concentrations. The $\text{Im } \chi^{(2)}$
25 spectrum of pure water (Figure 4 a and b, red line) exhibits a positive sharp peak at ~ 3700
26 cm^{-1} , a negative region ($\sim 3200 - 3650 \text{ cm}^{-1}$) and a slightly positive region ($\sim 3100 - 3200$
27 cm^{-1}). The sign of the $\text{Im } \chi^{(2)}$ is related to the orientation of the vibrational transition
28 dipole moment with respect to the surface plane. A negative value of $\text{Im } \chi^{(2)}$ is associated
29 with water molecules that are on average oriented with their dipoles pointing towards the
30 bulk, while a positive $\text{Im } \chi^{(2)}$ is associated with water molecules pointing away from the
31 bulk. Hydrogen-bonded OH groups at the water surface on average point down to the bulk,
32 causing the negative band at frequencies $\sim 3200 - 3650 \text{ cm}^{-1}$. The sharp positive feature at
33 $\sim 3700 \text{ cm}^{-1}$ is assigned to non-hydrogen bonded OH groups pointing into air. The positive
34 feature at frequencies $\sim 3100 - 3200 \text{ cm}^{-1}$ has been explained in different ways.^{17,18}

35
36
37
38
39
40
41
42
43
44
45
46
47
48
49
50 The $\text{Im } \chi^{(2)}$ spectra of TMABr and TEABr differ only slightly from the $\text{Im } \chi^{(2)}$ spectrum
51 of the pure water surface, in agreement with the intensity VSG data (Figure 4 a and b). In
52 contrast, the $\text{Im } \chi^{(2)}$ spectra of TPABr and TBABr are strongly concentration dependant.
53
54
55
56
57
58
59
60 At low concentrations of TPABr or TBABr ($\sim 0.001 \text{ M}$), the $\text{Im } \chi^{(2)}$ spectra are negative

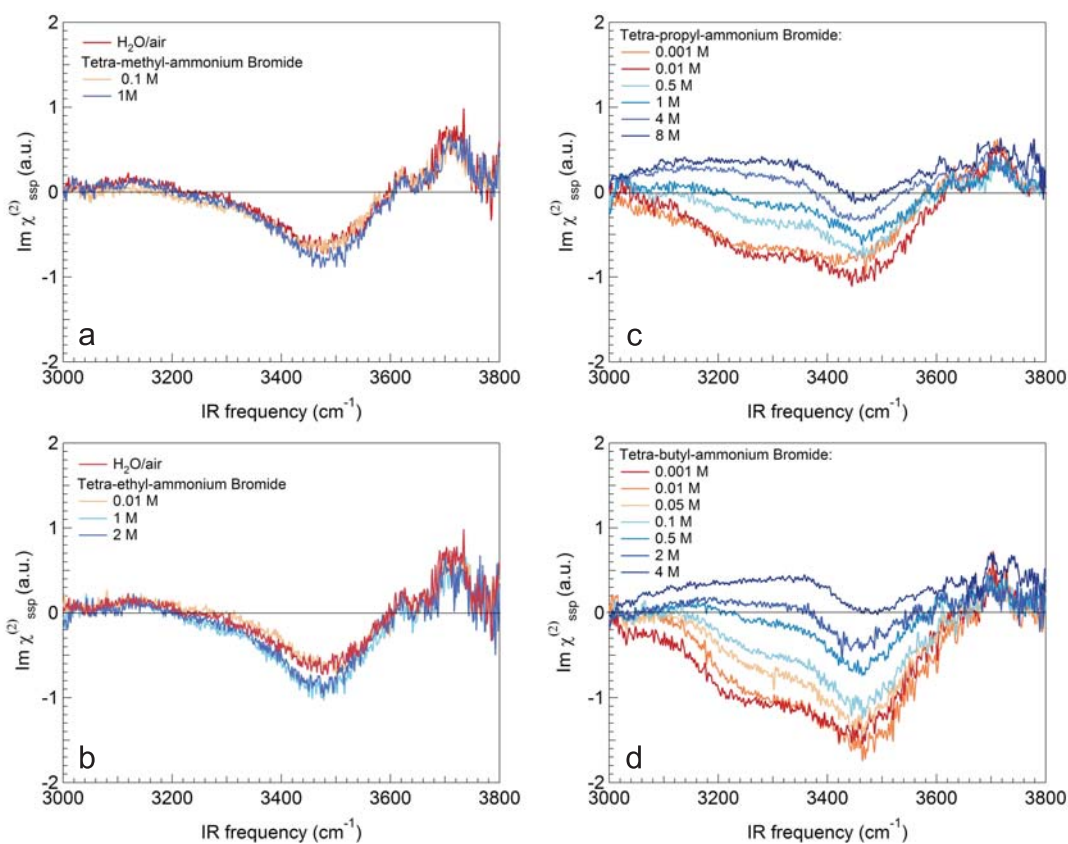


Figure 4: Imaginary $\chi^{(2)}$ spectra of (a) TMABr, (b) TEABr, (c) TPABr, and (d) TBABr at different concentrations (see legend).

throughout the hydrogen-bonded region, indicating that the water OH groups show a net orientation towards the bulk. Interestingly, the amplitude of this negative band decreases with increasing concentration. At high concentrations of TPABr (~ 1 M) and TBABr (~ 0.5 - 1 M) solutions the $\text{Im } \chi^{(2)}$ spectra become similar to the $\text{Im } \chi^{(2)}$ spectrum of the pure water surface. At extremely high concentrations of TPABr (~ 8 M) and TBABr (~ 4 M) the $\text{Im } \chi^{(2)}$ spectra acquire an overall positive sign, indicating that the O-H groups of the water molecules show a net orientation away from the water bulk. For solutions of tetra-propylammonium chloride (TPACl) we observe a very similar concentration dependence of the $\text{Im } \chi^{(2)}$ spectrum of the water band (see Figure SI2).

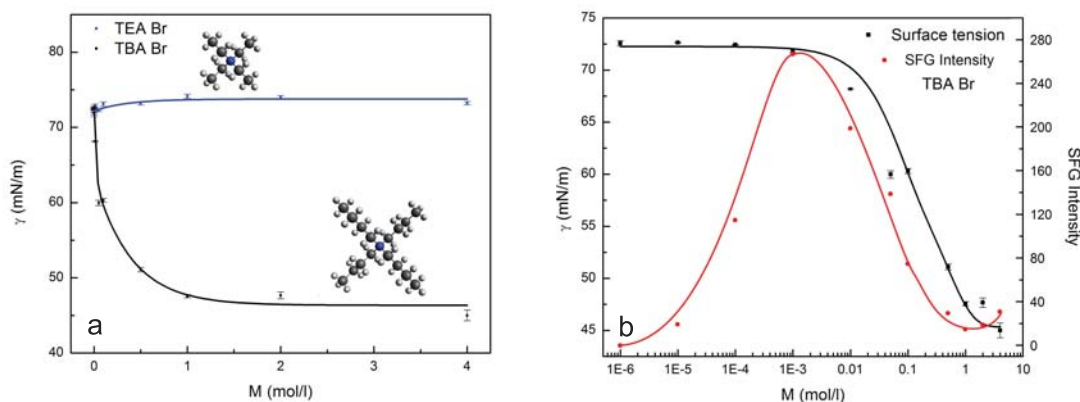


Figure 5: (a) Surface tension as a function of concentration for TEABr and TBABr solutions; (b) Surface tension and VSFGE intensity at 3200 cm^{-1} as a function of concentration for TBABr solutions. The lines are guides to the eye.

The intensity and heterodyne-detected VSFGE spectra of short-chain ($n = 1, 2$) TAABr salts are completely different from those of long-chain ($n = 3, 4$) TAABr salts. The VSFGE spectra of solutions of short chain TAA^+ cations are quite similar to the VSFGE spectrum of the surface of pure water, indicating a low surface propensity of these ions. Apparently, short chain TAA^+ cations are well solvated in bulk liquid water, which implies that the electrostatic interactions of the TAA^+ cations dominate over the hydrophobic interactions. In contrast, long chain TAA^+ cations are expelled from the bulk liquid leading to a high surface concentration. For long chain TAA^+ cations hydrophobic interactions between water

1
2
3 and the n-alkyl chains are hence more relevant than electrostatic interactions. This result
4 agrees with surface tension measurements.¹⁹ In Figure 5a we present the surface tension of
5 solutions of TEABr and TBABr as a function of concentration. It is observed that the surface
6 tension of TEABr remains constant (~ 72 mN/m) over the whole studied concentration range
7 of 0 - 4 M, whereas the surface tension of TBABr solutions strongly decreases with increasing
8 concentration, reaching a low value of ~ 45 mN/m for concentrations >1 M. In Figure 5b
9 we compare the concentration dependence of the surface tension of TBABr with that of
10 the intensity of the VSG signal at 3200 cm^{-1} . It is seen that at low concentrations the
11 VSG intensity strongly increases with concentration, while the surface tension is negligibly
12 affected. At concentrations >0.001 M both the VSG intensity and the surface tension
13 decrease, indicating a similar origin, i.e. the presence of a high density of TBA^+ and Br^-
14 ions in the interfacial region. Figure 5b thus clearly shows that the surface tension is not
15 representing the propensity of particular ions in the top molecular layers of the solution, but
16 rather the interfacial salt concentration probed over a much larger depth.
17
18
19
20
21
22
23
24
25
26
27
28
29
30
31

32 For solutions of short-chain TAA^+ ions, the increase of the concentration leads to a
33 small blue-shift of the hydrogen-bonded water band. This blue-shift indicates the presence
34 of relatively weak hydrogen bonds and can be explained from the increased contribution of
35 water O-H groups forming hydrogen bonds to Br^- ions. This result agrees with the work by
36 Allen and coworkers in which it was shown that the addition of halide salts to water leads to a
37 blue-shift of the intensity VSG spectrum.^{20,21} For TPABr and TBABr solutions the VSG
38 spectrum shows a strong red-shift at low concentrations, which obviously cannot be caused
39 by hydrogen bonding to Br^- ions. In previous studies we found that the hydrogen bonds
40 between water molecules become stronger at the interface of water and hydrophobic liquids
41 like hexane, heptane and polydimethylsiloxane.¹² A similar result was found in advanced
42 spontaneous Raman scattering studies of solutions of alcohols. In these studies it was shown
43 that the hydrogen-bond structure of water hydrating the alkyl chains of the alcohols is
44 enhanced in comparison to the hydrogen-bond structure of bulk liquid water.²² Hence, the
45
46
47
48
49
50
51
52
53
54
55
56
57
58
59
60

1
2
3
4
5
6
7
8
9
10
11
12
13
14
15
16
17
18
19
20
21
22
23
24
25
26
27
28
29
30
31
32
33
34
35
36
37
38
39
40
41
42
43
44
45
46
47
48
49
50
51
52
53
54
55
56
57
58
59
60

observed red-shift of the intensity and VSFG spectrum of solutions of TPABr and TBABr can be explained from the hydration of the hydrophobic alkyl chains of these ions near the solution surface. In addition to the red-shift, we observe an increase in intensity of the VSFG spectrum of TPABr and TBABr solutions in comparison to bulk liquid water. This intensity increase can be explained from the electric field that is created by the large concentration of hydrophobic cations at the surface and the Br^- ions that on average are located deeper down in the liquid. Br^- ions tend to have a somewhat higher concentration at the surface than in the bulk.²³⁻²⁵ However, in comparison to TPA^+ and TBA^+ ions the surface propensity of Br^- is weak. The separation of the positive TPA^+ and TBA^+ ions and the negative Br^- ions leads to an electric field pointing away from the surface, thereby orienting the water O-H groups towards the bulk phase, thus explaining the large negative value of $\text{Im } \chi^{(2)}$ of the water O-H band for low-concentration solutions of TPABr and TBABr. For the VSFG signal of the C-H vibrations the electric field effect is far less pronounced. In Figure 3a it is seen that the VSFG intensity of the C-H vibrations increases only gradually with increasing concentration. This strong difference in concentration dependence of the C-H and the water O-H signal can be explained from the fact that the water molecules possess a dipole moment, and thus strongly orient in the electric field created by TPA^+ and TBA^+ ions at the surface and Br^- ions deeper down in the liquid. The TPA^+ and TBA^+ ions do not possess a dipole moment as the alkyl chains are symmetrically (tetrahedrally) arranged around the N atom. For TPACl solutions we observe a similar concentration dependence of the $\text{Im } \chi^{(2)}$ spectrum of the water band, showing that Cl^- ions behave very similar to Br^- ions.

When the concentration of TPABr and TBABr is increased, the amplitude of the negative band decreases. This decrease can be explained from the decrease in distance between the centers of positive and negative charge in the interfacial region. As a result, there are less water molecules confined in between the TAA^+ and Br^- ions, and the VSFG signal decreases. At very high TPABr and TBABr concentrations, the TAA^+ cations and Br^- ions will form aggregated clusters at the solution surface, with a somewhat higher concentration of Br^-

ions deeper down in the solution. In Figure 6 we present a schematic picture of the interfacial configuration of the cations and anions at low and high concentrations of TPABr and TBABr. In the high-concentration regime there will be very few water molecules enclosed by the TAA⁺ and Br⁻ ions, and the VSG spectrum will become dominated by water molecules forming hydrogen bonds to the Br⁻ ions of the aggregated cation-anion layer at the surface. For these water molecules the O-H will have a net orientation away from the bulk, explaining the positive sign of the Im $\chi^{(2)}$ spectra in the high concentration regime. In addition, the hydrogen bonds to the Br⁻ ions are somewhat weaker than the hydrogen bonds between water molecules, thus explaining the blue-shift of the intensity and heterodyne detected VSG spectra of highly concentrated solutions of TPABr and TBABr.

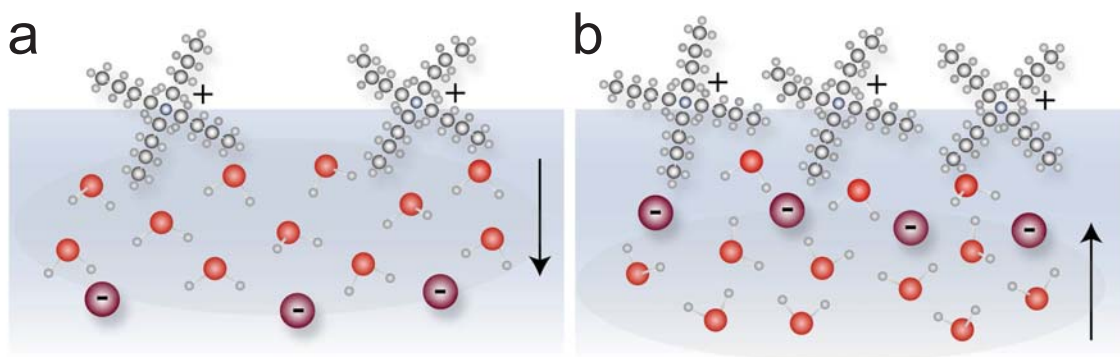


Figure 6: Schematic picture of the interfacial configuration of cations and anions at (a) low and (b) high concentrations of TPABr and TBABr.

Conclusions

We studied the surface properties of solutions of tetra-*n*-alkylammonium bromide salts using intensity and heterodyne detected vibrational sum-frequency generation (VSG) spectroscopy. We observe that short-chain tetra-*n*-alkylammonium bromides ($n = 1, 2$) behave like simple inorganic salts. The TAA⁺ ions show little surface propensity. As a result, the

1
2
3 VSG spectra of short-chain tetra-n-alkylammonium bromides ($n = 1, 2$) are similar to the
4 VSG spectrum of pure liquid water. A slight blue shift of the spectrum is observed that can
5 be explained from the contribution of water molecules forming hydrogen bonds to the Br^-
6 ions. For long-chain tetra-n-alkylammonium bromides ($n = 3, 4$) we observe a very different
7 VSG spectrum, due to the high surface propensity of the tetra-propyl-ammonium and tetra-
8 butyl-ammonium cations. At low bulk concentrations, the VSG spectra are dominated by
9 hydrophobic hydration effects, leading to a red-shift of the response of hydrogen-bonded
10 water molecules. In addition the amplitude of the VSG spectrum is strongly enhanced
11 due to the orienting electric field that is created by the separation of the center of positive
12 charge associated with the positive tetra-n-alkylammonium (TAA^+) ions at the surface and
13 the center of negative charge associated with the Br^- ions deeper down in the solution. At
14 high concentrations, the TAA^+ and Br^- ions form aggregated clusters at the solution surface
15 and the VSG spectrum is dominated by water molecules forming hydrogen bonds to the
16 Br^- ions of these clusters.
17
18
19
20
21
22
23
24
25
26
27
28
29
30
31
32
33

34 Acknowledgement

35
36 This work is part of the research program of the "Stichting voor Fundamenteel Onderzoek
37 der Materie (FOM)", which is financially supported by the "Nederlandse organisatie voor
38 Wetenschappelijk Onderzoek (NWO)". The work was performed within the framework of a
39 FOM Industrial Partnership Program with Top-institute Wetsus for water research and is
40 also financially supported by Wetsus.
41
42
43
44
45
46
47
48

49 Supporting Information Available

50
51 In the supporting information we show linear IR spectra of TEABr and TBABr at different
52 concentrations and Imaginary $\chi^{(2)}$ spectra of TPACl at different concentrations.
53
54

55 This material is available free of charge via the Internet at <http://pubs.acs.org/>.
56
57
58
59
60

References

- (1) Ball, P. Water as an Active Constituent in Cell Biology. *Chem. Rev.* **2008**, *108*, 74–108.
- (2) Lum, K.; Chandler, D.; Weeks, J. D. Hydrophobicity at Small and Large Length Scales. *J. Phys. Chem. B* **1999**, *103*, 4570.
- (3) Chandler, D. Interfaces and the Driving Force of Hydrophobic Assembly. *Nature* **2005**, *437*, 640–647.
- (4) Frank, H. S.; Evans, J. W. Free Volume and Entropy in Condensed Systems. 3. Entropy in Binary Liquid Mixtures; Partial Molar Entropy in Dilute Solutions; Structure and Thermodynamics of Aqueous Electrolytes. *J. Chem. Phys.* **1945**, *13*, 507–532.
- (5) Wen, W.-Y. Structural Aspects of Aqueous Tetraalkylammonium Salt Solutions. *J. Sol. Chem.* **1973**, *2*, 253–276.
- (6) Soper, A.; Finney, J. Hydration of Methanol in Aqueous-Solution. *Phys. Rev. Lett.* **1993**, *71*, 4346–4349.
- (7) Dixit, S.; Crain, S.; Poon, W.; Finney, J.; Soper, A. K. Molecular Segregation Observed in a Concentrated Alcohol-Water Solution. *Nature* **2002**, *416*, 829–832.
- (8) Huang, N.; Schlesinger, D.; D.Nordlund; Huang, C.; Tyliczszak, T.; Weiss, T. M.; Acremann, Y.; Pettersson, L. G. M.; Nilsson, A. Microscopic Probing of the Size Dependence in Hydrophobic Solvation. *J. Chem. Phys.* **2012**, *136*, 074507–7.
- (9) Nihonyanagi, S.; Mondal, J. A.; Yamaguchi, S.; Tahara, T. Structure and Dynamics of Interfacial Water Studied by Heterodyne-Detected Vibrational Sum-Frequency Generation. *Annu. Rev. Phys. Chem.* **2013**, *64*, 579–603.
- (10) Ji, N.; Ostroverkhov, V.; Tian, C. S.; Shen, Y. R. Characterization of Vibrational Resonances of Water-Vapor Interfaces by Phase-Sensitive Sum-Frequency Spectroscopy. *Phys. Rev. Lett.* **2008**, *100*, 096102.

- 1
2
3
4
5
6
7
8
9
10
11
12
13
14
15
16
17
18
19
20
21
22
23
24
25
26
27
28
29
30
31
32
33
34
35
36
37
38
39
40
41
42
43
44
45
46
47
48
49
50
51
52
53
54
55
56
57
58
59
60
- (11) Shen, Y. R. Phase-Sensitive Sum-Frequency Spectroscopy. *Annu. Rev. Phys. Chem.* **2013**, *64*, 129–50.
- (12) Strazdaite, S.; Versluis, J.; Backus, E. H.; Bakker, H. J. Enhanced Ordering of Water at Hydrophobic Surfaces. *J. Chem. Phys.* **2014**, *140*, 054711.
- (13) Strazdaite, S.; Versluis, J.; Bakker, H. J. Water Orientation at Hydrophobic Interfaces. *J. Chem. Phys.* **2015**, *143*, 084708.
- (14) Sovago, M.; Campen, R. K.; Wurpel, G. W. H.; Muller, M.; Bakker, H. J.; Bonn, M. Vibrational Response of Hydrogen-Bonded Interfacial Water is Dominated by Intramolecular Coupling. *Physical Review Letters* **2008**, *100*, 173901.
- (15) Bergstrom, P.-A.; Lindgren, J.; Kristiansson, O. An IR Study of the Hydration of Ca^{2+} , NO_3^- , I^- , Br^- , Cr^{3+} , and SO_4^{2-} Anions in Aqueous Solution. *J. Phys. Chem.* **1991**, *95*, 8575–8580.
- (16) Hidaka, F.; Kanno, H. Raman OD Stretching Spectral Differences between Aqueous and Alcoholic Tetraalkylammonium Chloride Solutions. *Chem. Phys. Lett.* **2003**, *379*, 3-4, 216–222.
- (17) Pieniazek, P. A.; Tainter, C. J.; Skinner, J. L. Interpretation of the Water Surface Vibrational Sum-Frequency Spectrum. *J. Chem. Phys.* **2011**, *135*, 044701.
- (18) Ishiyama, T.; Morita, A. Vibrational Spectroscopic Response of Intermolecular Orientational Correlation at the Water Surface. *J. Phys. Chem. C* **2009**, *113*, 16299–16302.
- (19) Tamaki, K. Surface Activity of Tetra-n-Alkylammonium Halides in Aqueous Solutions. *Bull. Chem. Soc. Jpn.* **1974**, *47(11)*, 2764–2767.
- (20) Liu, D.; Ma, G.; Levering, L.; Allen, H. C. Vibrational Spectroscopy of Aqueous Sodium Halide Solutions and Air-Liquid Interfaces: Observation of Increased Interfacial Depth. *J. Phys. Chem. B* **2004**, *108(7)*, 2252–2260.

- 1
2
3
4 (21) Verreault, D.; Allen, H. C. Bridging the Gap between Microscopic and Macroscopic
5 Views of Air/Aqueous Salt Interfaces. *Chem. Phys. Lett.* **2013**, *586*, 1–9.
6
7
8
9 (22) Davis, J. G.; Gierszal, K. P.; Wang, P.; Ben-Amotz, D. Water Structural Transformation
10 at Molecular Hydrophobic Interfaces. *Nature* **2012**, *491*, 582–585.
11
12
13 (23) Jungwirth, P.; Tobias, D. J. Specific Ion Effects at the Air/Water Interface. *Chem. Rev.*
14 **2006**, *106*, 1259–1281.
15
16
17
18 (24) Ishiyama, T.; Morita, A. Molecular Dynamics Study of Gas-Liquid Aqueous Sodium
19 Halide Interfaces. I. Flexible and Polarizable Molecular Modeling and Interfacial Prop-
20 erties. *J. Phys. Chem. C* **2007**, *111*, 721–737.
21
22
23
24
25 (25) Nihonyanagi, S.; Yamaguchi, S.; Tahara, T. Counterion Effect on Interfacial Water
26 at Charged Interfaces and Its Relevance to the Hofmeister Series. *J. Am. Chem. Soc.*
27 **2014**, *136(17)*, 6155–6158.
28
29
30
31
32
33
34
35
36
37
38
39
40
41
42
43
44
45
46
47
48
49
50
51
52
53
54
55
56
57
58
59
60

Graphical TOC Entry

